Photoproduction of π^0 Mesons from He^3 with 340-MeV Bremsstrahlung

M. BLECHER* AND A. O. HANSON
Physics Department, University of Illinois, Urbana, Illinois
(Received 3 January 1969)

Differential cross sections for the coherent photoproduction of π^0 mesons from He^3 [$He^3(\gamma, \pi^0)He^3$] were measured for recoil angles of 20°, 30°, 40°, and 50° and were found to be 2–8 μb/sr, 5–25 μb/sr, 17–56 μb/sr, and 17–84 μb/sr, respectively. A gaseous He^3 target at 20.4°K was irradiated by 340-MeV bremsstrahlung, and He^3 recoils were observed with silicon semiconductor detectors. At least one γ ray from the pion decay was detected with a photon shower counter. A coincidence triggered an oscilloscope on which all pulses were displayed and photographed. The experimental cross sections are compared with those obtained by various impulse-approximation calculations. Although the calculations depend on the manner of specifying the energy and momentum dependence of the photon-nucleon amplitudes in the He^3 nucleus, a calculation assuming that the three nucleons were initially at rest accounts for most of the measurements.

INTRODUCTION

THIS measurement of the $He^3(\gamma, \pi^0)He^3$ cross section is a part of a study of photon reactions in light nuclei. It is similar to a previous measurement of the $He^3(\gamma, \pi^+)H^3$ reaction by O'Fallon, Koester, Smith, and Yavin.[1] The present work, however, uses higher photon energies, which extend up to the $(\frac{3}{2}, \frac{3}{2})$ pion-nucleon resonance. The production of π^0 rather than π^+ mesons simplifies the interpretation of the reaction, since the initial and final nuclear states are the same.

The cross sections found in this work are compared with those calculated using the known photon-pion production amplitudes for free nucleons in an impulse approximation reduced by the experimentally determined form factors. Although some of the calculations account for the observations reasonably well, they give different cross sections for different simplified ways of specifying the initial and final energy and momentum of the nucleon in the He^3 nucleus. A more definitive calculation is required before differences between observed and calculated values can be discussed with confidence.

DESIGN OF THE EXPERIMENT

The arrangement of equipment is shown in Fig. 1. 340-MeV x rays originating at the internal betatron target were defined to form a rectangular beam 1 in.$\times$ 2 in. at the He^3 gas target. Charged particles were eliminated with two sweeping magnets. The He^3 gas target was cooled to liquid-hydrogen temperature and was maintained at a pressure slightly above 1 atm.

Events from the $He^3(\gamma, \pi^0)He^3$ reaction were identified by coincidences between signals from He^3 recoils in the semiconductor-detector telescopes and a signal from the π^0 γ rays in the shower counter.

When the timing circuitry indicated a coincidence, the pulse heights from the detectors were displayed on an oscilloscope and photographed. These photographs comprise the experimental data.

BEAM COLLIMATION

One side of the target chamber is flattened to permit the shower counter to be within 3 in. of the target, where the probability for intercepting at least one of the two decay photons is about 96%. When the shower counter was first placed in that position, however, the counting rate was very high. In order to reduce the background due to secondary x rays and electrons reaching the shower detector, two collimators, in addition to the regular, primary, and secondary collimators, were used. These were tapered so that no x rays coming from previous collimators could strike their inner walls, and were strategically placed so as to block any scattered x rays which could strike any part of the target chamber. The alignment was critical, and it was found that the background rate was sensitive to movements of 0.005 in. in the position of the x-ray target or in the position of the collimators.

The x-ray yield was monitored with a quantameter. Its sensitivity was checked experimentally, compared with an N.B.S.-type monitor,[2] and found to be 1.36 μC/J in agreement with other calibrations.[3]

CRYOGENIC TARGET

The liquid-hydrogen-cooled He^3 gas target was the same one described in the previous experiment.[1] Basically, it was a cylinder 1.25 in. in diameter with 0.0015-in. Mylar walls. It was surrounded completely by a copper shield, wrapped with aluminum foil, at liquid-hydrogen temperature. Windows in this shield for the entrance and exit of the x-ray beam as well as for the He^3 recoils were covered with aluminized 0.00015-in. Mylar. Tests using the ideal gas law and a carbon resistor indicated that the mean temperature of the He^3 gas was 20.8$\pm$0.4°K.

The base, with one flat side to accommodate the shower counter and a housing for the semiconductor telescopes, was built specifically for this experiment.

* Present address: Virginia Polytechnic Institute, Blacksburg, Va.

[1] J. R. O'Fallon, L. J. Koester, Jr., J. H. Smith, and A. I. Yavin, Phys. Rev. 141, B889 (1966).

[2] W. P. Swanson, R. A. Carrigan, Jr., and E. L. Goldwasser, Rev. Sci. Instr. 34, 538 (1963).

[3] R. Gomez, J. Pine, and A. Silverman, Nucl. Instr. Methods 24, 429 (1963).

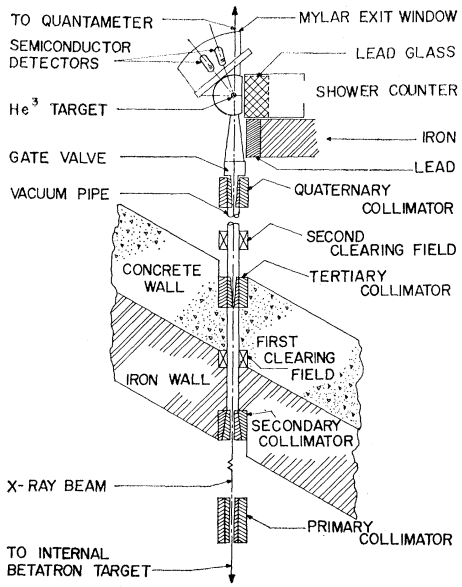

FIG. 1. Experimental arrangement.

SEMICONDUCTOR TELESCOPES

The semiconductor telescopes were housed in a removable addition to the target chamber, which could be isolated from the target vacuum by means of a special vacuum gate. Portholes for mounting the telescopes were cut into the top of the housing at 20° and 40°, and into the bottom at 30° and 50°.

Two semiconductor telescopes were in use at all times during the experiment. Each telescope consisted of three Ortec detectors of increasing thickness as listed in Table I. The brass cylinders holding the telescopes were cooled by means of a small Freon refrigerator unit so as to reduce all reverse currents below 0.2 μA. The bias voltage was sufficient to totally deplete the detectors. Each detector was followed by a charge-sensitive preamplifier, and the step output was taken as proportional to the energy lost in each detector. The over-all calibration of each detector was checked routinely by observing the pulse-height spectrum of a few 5.3-MeV α particles per hour from a small amount of polonium 210 deposited on the surface of each detector.

The experiment was begun with the 43-μ detector in the telescope at 40°. Photographs were obtained with pulses in the 122-μ and 496-μ SSD's (Solid-State detectors), which looked like He^3, but no pulse in the 43-μ SSD. It was suspected that part of the latter's supposed active area was dead, and on testing with a well collimated beam these suspicions were confirmed. The 49-μ SSD was then substituted for the 43-μ SSD.

SHOWER COUNTER

The counter used for detecting the π^0 photons consisted of a lead glass cylinder with a radiation length of 1 in. It was 12 in. in diameter and 7 in. thick and placed as shown in Fig. 1. Four 7046 photomultiplier tubes viewed the Čherenkov light. The assembly was enclosed in a light-tight container, and surrounded by a Mumetal magnetic shield. Two types of light signals were provided on the front of the counter. One was a luminescent diode (Monsanto MVE 100), which was fired from a mercury switch pulser for checking the over-all electronic system. The other was radioactive Cs^{137} on a piece of scintillator, which was covered by a movable opaque shield. This source was used to check the gain stability of each of the four photomultiplier tubes. Each phototube anode and dynode went directly to emitter followers with input impedances of about 500 Ω and outputs into 50-Ω lines. These emitter followers greatly improved the signal from the individual phototubes and increased the reliability of the subsequent circuitry.

ELECTRONICS

The electronic system for selecting and displaying events is shown schematically in Fig. 2. Note that each semiconductor was followed by a charge-sensitive preamplifier, whose output was shaped and clipped before being split into two branches. One branch trips a trigger circuit T, and the other, after an appropriate delay, enters one of two mixer circuits, displaying signals on the two beams of a Tektronix 551 oscilloscope. If any one of the six semiconductor triggers are tripped, there will be a logic signal from the OR circuit into one side of the master coincidence circuit MC. A logic signal as well as an analog signal are also taken from the photon shower detector. Since the level of the Čherenkov-light signals in the individual photomultiplier tubes are below much of the tube noise, reliable indications of a photon shower were obtained by requiring coincident signals from at least two of the four photomultipliers within 20 nsec. The output of this 2-of-4 coincidence was routed to the master coincidence where a coincidence between this pulse and one from any of the six semiconductors within 300 nsec triggers the oscilloscope sweep.

The analog signal from the shower detector was

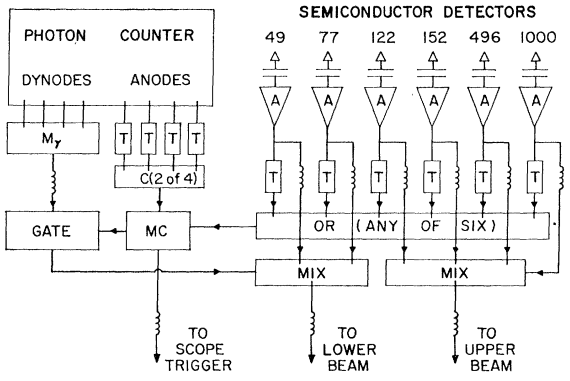

FIG. 2. Block diagram of the electronics.

obtained from the photomultiplier dynodes which were added by the mixer circuit M_γ. Since this signal was very noisy, it could not be added continuously to those of the thin detectors without spoiling their energy resolution. The γ signal O_γ was, therefore, passed through a fast linear gate G, which was opened for only 300 nsec leaving the rest of the 1500-nsec trace for the semiconductor trace without this noise.

A sketch showing the display from an event in one of the telescopes is shown in Fig. 3. The pattern for each telescope is uniquely defined by the delays and clipping times associated with the pulses. The photon gate is seen with the photon signal within it.

DATA ANALYSIS

Photographs such as those shown in Fig. 3 were scanned, and those events in which at least 1 MeV was deposited in the thin detector or at least 4 MeV in all detectors were selected for measurement with a Hydel digitized measuring machine. The time delays T_A, T_B, and T_C as well as the pulse widths D_A, D_B, and D_C serve to identify the telescope receiving the recoil. The pulse heights P_1, P_2, and P_3 determine the energy lost in each detector.

The punch cards recording the coordinates of various points on the film were processed by a computer and provided a printed summary which identified the event, the energies lost in each detector, and the total energy of the recoil. The computer then used the total energy and the range-energy relation to compute the energies deposited in each of the detectors on the assumption that it was a triton, a He^3, or a He^4 recoil. The event was accepted if the losses calculated for either He^3 or He^4 were in better agreement with the observed energies than that for a triton. If not, the event was discarded.

The over-all energy resolution was not sufficient to separately identify He^3 and He^4, but since there was no He^4 in the target gas, all He^4 recoils must come from the Mylar container or nearby materials. The net He^3 spectrum was found by including all $Z=2$ events obtained with the target filled with He^3 and subtracting all $Z=2$ events obtained with the target evacuated. The kind of identification which was achieved in these telescopes can be seen in Fig. 4, where the total energy of each of the measured events of a particular run are shown as a function of the energy lost in the first detector. Since other reactions such as Compton scattering, which could lead to real coincidences between He^3 recoils and secondary photons, were estimated to contribute less than 1% of the neutral pion reaction, they were neglected.

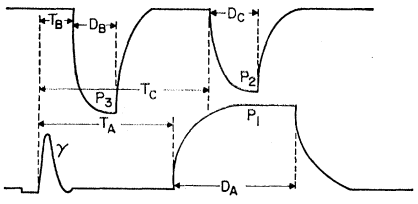

FIG. 3. Display of pulse heights on the dual-beam oscilloscope.

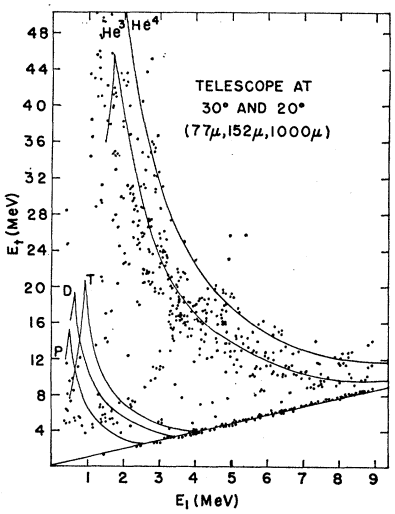

FIG. 4. Distribution of events in which the total energy lost in all three detectors of the forward semiconductor telescope is given by the ordinate with the energy lost in the first detector as the abscissa.

A summary of the number of $Z=2$ events found in specified energy bins from filled and empty target runs is found in Table II. It can be seen that a large fraction of the events at 20° and 30° are background events. The systematic and the statistical uncertainties associated with this background greatly increases the possible errors in the cross sections at these angles.

The set number of recoils counted in a particular bin of recoil energy $C_i(E_R, \Delta E_R)$ when combined with other measurements are used to obtain a differential cross section by the usual relation

$$C_i(E_R, \Delta E_R) = W_\gamma F_i(E_\gamma, \Delta E_\gamma) n (d\sigma/d\Omega) \Delta\Omega \tau_d \epsilon_s,$$

where W_γ is the total photon energy flux in J passing through the He^3 target during a particular run as determined by the quantameter. $F_i(E_\gamma, \Delta E_\gamma)$ is the number of photons per J of total photon flux in a particular energy bin of width ΔE_γ and energy E_γ corresponding to the recoil energy bin width ΔE_R and energy E_R. This number is evaluated from the integrated bremsstrahlung formula given by Schiff.[4] n is the effective number of He^3 nuclei per cm^2 in the target as traversed by the photon beam. $\Delta\Omega$ is the effective solid angle subtended at the target by the first semiconductor detector. τ_d is a dead-time correction factor which accounts for the fraction of the time the equipment was insensitive when the camera film was in motion. This time factor was always greater than 0.94. The final factor ϵ_s represents the efficiency with which at least one of the π^0 photons associated with the He^3 recoils will be detected by the shower detector. This factor was evaluated

[4] L. I. Schiff, Phys. Rev. **83**, 252 (1951).

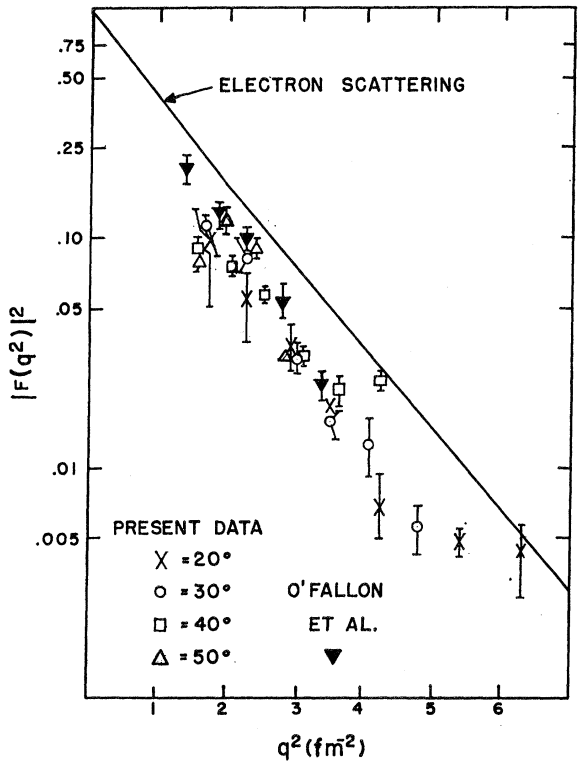

FIG. 5. Form factors obtained from the experimental cross sections divided by calculated free-nucleon values using the same nucleon vector momentum transfer as for the nuclear system. The line represents the form factor as determined from electron scattering data.

by means of a Monte Carlo computer program simulating 10 000 photoproduction events for each bin. For the geometry used, this efficiency ϵ_s was always greater than 0.96.

In the actual calculations, the coefficient of $d\sigma/d\Omega$ was determined by a Monte Carlo program which began by choosing a random point in the irradiated portion of the gas target, selecting a random energy within an energy bin, and keeping a record of the fraction of events which were detected simultaneously by the recoil telescope and the shower detector. These cross sections and the associated statistical errors are listed in column 7 of Table II and are plotted in Fig. 5. The square of the momentum transfer q is included in the table for convenience in discussing the form-factor dependence. In column 6, q^2 is divided by $(10^{13}\hbar)^2$ so as to express the momentum transfer in reciprocal Fermis squared.

INTERPRETATION OF RESULTS

Previous analyses[1,5] have confirmed, at least qualitatively, that photopion production from complex nuclei can be described in terms of the photoproduction amplitudes from free nucleons. The accurate verification of this assumption or the discernment of quantitative discrepancies would be important in understanding the role of the pion in nuclear structure. As in a previous work,[1] a calculation based on a simple impulse approximation is used in discussing the experimental cross sections. It is assumed that the amplitude for the experimental reaction $He^3(\gamma,\pi^0)He^3$ is an appropriate sum of Chew-Goldberger-Low-Nambu (CGLN[6]) amplitudes for photoproduction from free nucleons, that the pion may be treated as a plane wave, and that the wave function for the He^3 nucleus is composed of a completely symmetric spatial S state ψ_{He^3} with spin and isospin states, one of which is symmetric and the other antisymmetric.

In this model, the center-of-mass differential cross section for $He^3(\gamma,\pi^0)He^3$ can be written as

$$d\sigma/d\Omega^*=\phi_n(|A_n|^2+9|B_n|^2)\phi_{He^3}|F(q^2)|^2_{He^3}, \quad (1)$$

where

$$\phi_n=[W_iW_f/kE_iE_fE_\pi]_n, \quad (2)$$

$$\phi_{He^3}=[P_\pi E_iE_fE_\pi/W_iW_f]_{He^3}, \quad (3)$$

$$F(q^2)_{He^3}=\int\exp(i\mathbf{q}\cdot\mathbf{r}_1)\,|\psi_{He^3}|^2 d\mathbf{r}_1 d\mathbf{r}_2 d\mathbf{r}_3. \quad (4)$$

The kinematical quantities comprising ϕ_n and ϕ_{He^3} are to be evaluated in the center-of-mass frames of the reactions $n(\gamma,\pi^0)n$ and $He^3(\gamma,\pi^0)He^3$, respectively. Specifically, W_i and W_f are the total initial and final energies of the system, k is the photon energy, E_i and E_f are the initial and final energies of the target, and E_π and P_π are the energy and momentum of the pion. A_n and B_n are the spin-flip and non-spin-flip CGLN amplitudes for the process $n(\gamma,\pi^0)n$ and are functions of the kinematical variables comprising ϕ_n. Their respective coefficients 1 and 9 reflect the fact that $B_p=B_n$, that only the neutron contributes to the spin-flip term, and that all the nucleons contribute to the non-spin-flip term. $F(q^2)_{He^3}$ is the matter form factor of

TABLE I. Semiconductor detector telescopes.

Telescope angle (deg)	Detector	Thickness (μ)	Active area (mm^2)	α stopping energy (MeV)
20 and 30	A	77	200	11.4
	B	152	300	16.5
	C	1000	300	50.0
40 and 50	A	43	200	7.6
		49	200	8.0
	B	122	300	15.0
	C	496	300	33.8

[5] V. V. Balashov, G. Ya. Korenman, and T. S. Macharadze, Yadern Fiz. 1, 668 (1965) [English transl.: Soviet J. Nucl. Phys. 1, 479 (1965)].

[6] G. Chew, M. Goldberger, F. Low, and Y. Nambu, Phys. Rev. 106, 1345 (1957).

TABLE II. Experimental results.

E_{recoil} (MeV)	E_{photon} (MeV)	C_{data}	$C_{background}$	C_{He^3}	c.m. (Momentum transfer)^2 (fm^{-2})	$d\sigma/d\Omega_{He^3}$ (μb/sr)	θ_{π^0}* (deg)	$d\sigma/d\Omega$* (μb/sr)
				$\theta_{He^3}=20°$				
11.55±1.85	184±10	526	460	66	1.7±0.3	4.9±2.4	128	0.8±0.4
15.40±2.00	201±10	315	248	67	2.3±0.3	5.3±1.9	131	1.0±0.3
19.70±2.30	220±10	237	153	84	2.9±0.3	6.9±1.7	134	1.4±0.3
24.40±2.40	240±10	135	50	85	3.6±0.3	7.8±1.4	135	1.6±0.3
29.20±2.40	258±10	102	62	40	4.3±0.3	4.2±1.3	136	0.9±0.3
36.50±4.90	285±18	101	50	51	5.4±0.5	3.1±0.7	137	0.7±0.2
46.40±5.00	321±18	60	33	27	6.3±0.5	2.1±0.8	137	0.5±0.2
				$\theta_{He^3}=30°$				
11.55±1.85	199±10	269	176	93	1.7±0.3	14.1±3.2	104	2.8±0.6
15.40±2.00	219±10	296	148	148	2.3±0.3	24.3±3.4	109	5.2±0.6
19.70±2.30	240±10	189	110	110	2.9±0.3	18.7±2.8	112	4.3±0.6
24.00±2.00	259±9	100	60	60	3.5±0.3	13.3±3.7	113	3.2±0.9
28.30±2.30	278±10	83	52	52	4.1±0.3	11.3±2.4	114	2.8±0.6
33.50±2.90	300±11	58	27	27	4.8±0.3	4.9±1.6	115	1.2±0.4
				$\theta_{He^3}=40°$				
11.20±1.50	223±8	517	275	242	1.6±0.25	30.4±3.6	85	7.2±0.9
14.20±1.50	241±8	498	145	353	2.1±0.25	49.6±3.7	90	12.6±0.9
17.40±1.70	260±10	492	96	396	2.6±0.3	56.0±3.4	91	14.9±0.9
21.05±1.95	281±10	452	104	348	3.1±0.3	33.8±2.4	92	9.3±0.7
24.90±1.90	302±10	261	79	182	3.7±0.3	20.6±2.1	93	5.9±0.6
29.60±2.40	325±10	195	54	141	4.3±0.3	16.7±1.8	94	4.9±0.5
				$\theta_{He^3}=50°$				
11.20±1.50	270±9	466	122	344	1.6±0.25	62.8±4.4	66	19.4±1.4
13.80±1.20	289±8	379	40	339	2.0±0.25	84.2±5.1	68	27.3±1.7
16.20±1.20	305±8	238	37	201	2.4±0.25	57.8±4.6	69	19.3±1.5
19.70±2.30	330±10	110	26	84	2.9±0.3	16.6±2.3	71	5.7±0.8

He^3 and is only a function of the square of the momentum transferred to the He^3 nucleus. In principle, the quantity $\phi_n(|A_n|^2+9|B_n|^2)$ should remain under the integral. To facilitate the calculation, we have followed O'Fallon[1] and assumed that it can be removed from the integral.

The experimental reaction $He^3(\gamma,\pi^0)He^3$ contains two particles in both the initial and final states. It is assumed that the target is at rest in the laboratory and the direction of the incident photon is known. Conservation of energy and momentum enables us to completely specify the experimental kinematics if the values of at least two kinematical variables are known. The measured values of the energy and angle of the recoil He^3 are then sufficient to determine the experimental kinematics.

In Eq. (1), however, there are terms (ϕ_n, A_n, B_n) which do not depend on the experimental kinematics, but on the kinematics for the photoproduction from free nucleons $[n(\gamma,\pi^0)n]$. The problem arises as to how to specify the kinematics for the latter case.

In the previous work, the nucleon kinematics were defined by first assuming that the target nucleons were at rest and that the direction of the incident photon is known. The center-of-mass photon energy, pion energy, and pion angle, which must be specified in evaluating the photopion amplitudes for the photon-nucleon system, were rather arbitrarily evaluated in two different ways.

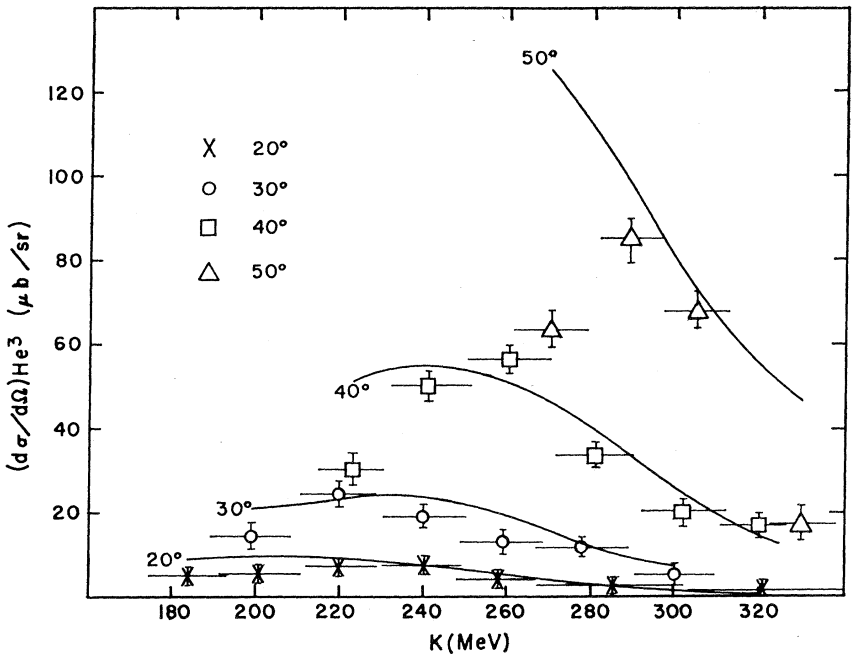

FIG. 6. Experimental laboratory cross sections for the observation of He^3 recoils are shown as a function of the laboratory photon energy. The solid lines are the theoretical cross sections as calculated using the laboratory pion, photon, and recoil vector momenta as the pion, photon, and nucleon vector momenta in the photon-nucleon system. The form factor used in this calculation was that obtained from electron scattering.

The first assumed that the laboratory photon energy in the nucleon system was the same as the laboratory photon energy defined by the He^3 recoil energy and angle, and that the magnitude of the momentum transfer to the recoil nucleon was that of the recoil nucleus. The rest of the kinematics were determined by using the conservation of energy and momentum in the photon-nucleon system. The second method specified that the momentum transfer, magnitude, and direction of the nucleon be that of the observed nuclear recoil. Again the conservation of energy and momentum in the photon-nucleon system determined the rest of the kinematics. In that experiment these assumptions led to cross sections which were not significantly different. At the higher energies of this experiment the first assumption, when applied to the 20° data, could not be carried out consistently so that only the second assumption was used in comparing the two experiments.

The comparison is facilitated by dividing the experimental center-of-mass cross sections by the calculated values of $\phi_n[A_n|^2+9|B_n|^2]\phi_{He^3}$ to obtain experimental values for the squared form factors $|F(q^2)|^2$. Points obtained in this way are shown in Fig. 5 with the average of the points from the $He^3(\gamma,\pi^+)H^3$ experiment. The deviations from the expected form-factor curve might be interpreted as being due to approximations in the evaluation of the theoretical expression or indicating the need for corrections to the theory. The line in this figure represents the squared form factor as obtained from electron scattering according to the relation[7]

$$F(q^2)=2F_{He^3}(q^2)/[2F_p(q^2)+F_n(q^2)], \quad (5)$$

[7] L. I. Schiff, Phys. Rev. **133**, B802 (1964).

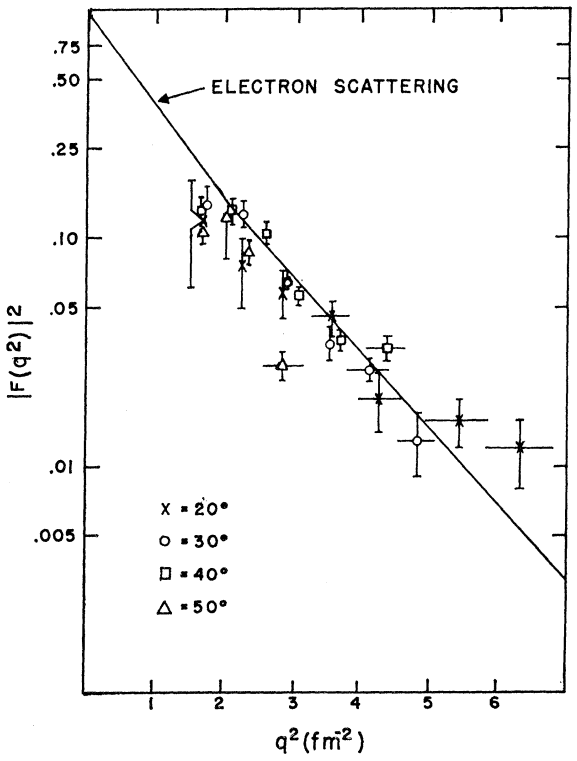

FIG. 7. Form factors as determined from the experimental data by the same calculation as used in Fig. 6. The same electron scattering form factor as in Fig. 5 is included to show the differences between these values and the previous ones shown in Fig. 5.

where $F_{He^3}(q^2)$, $F_p(q^2)$ and $F_n(q^2)$ are the charge form factors of He^3, the proton, and the neutron as tabulated by Srivastava.[8] In the limit of zero q, we have $F_{He^3}=1$, $F_p=1$, and $F_n=0$, so that F approaches 1 in this limit. It can be seen that the experimental results are in reasonable agreement with each other but lie below the line by factors which can be seen to increase from 1.5 to more than 3 as the momentum transfer increases to give a q^2 of about 6 F^{-2}.

A number of other kinematical assumptions were made in calculating the cross sections to be expected from theory. These calculations gave widely differing results. One of these which gives reasonable agreement with the experimental values is the one in which the laboratory vector momentum of the photon, that of the pion, and that of the recoil nucleon are set equal to those of the photon, pion and recoil nucleus of the $He^3(\gamma, \pi^0)He^3$ laboratory system. In this case, we retain momentum conservation in the photon-nucleon system. However, because the nucleon mass is approximately one-third the He^3 mass, we no longer have energy conservation in the photon-nucleon system. The energy violation in the center-of-mass system prevents the amplitudes from reaching the usual resonant values and results in reduced maximum cross sections. These cross sections together with those determined experimentally are shown in Fig. 6. It can be seen that the calculated curves [using $F(q^2)$ as defined by Eq. (5)] represent the experimental data quite well except for the extreme values which are most subject to systematic errors. The same experimental points when divided by corresponding calculated values except for the form factor are shown with the line representing the form factor in Fig. 7. It can be seen that in this case there is no general disagreement between these points and the line expected from electron scattering.

It appears that the simple impulse approximations as used here and in the previous work are very useful in obtaining estimates of the magnitudes of the cross sections for photopion production from nuclei and to discuss some of their distinctive features. It might be hoped that one could identify effects associated with the suppression of pion production in nuclei as well as those associated with scattering and absorption of the outgoing pion, but it seems that the ambiguities resulting from the manner in which the kinematics are specified are too large at the energies used in this work. It would be necessary, therefore, to have better calculations which use the nucleon wave functions in the He^3 nucleus in evaluating the effective photon-nucleon amplitudes before a quantitative discussion of discrepancies between experimental and calculated values would be meaningful.

[8] B. K. Srivastava, Phys. Rev. **133**, B545 (1964).

ACKNOWLEDGMENTS

The authors would like to thank Professor L. J. Koester, Jr., for advice concerning the experimental aspects of this work and Professor D. G. Ravenhall and Professor R. L. Schult for advice concerning the theoretical aspects of this work. We are grateful to Don Vermillion and the betatron staff for help in setting up and running the experiment and to Steve Kiergan, James Murphy, and John Staples for assistance during various phases of the experiment.